J Mater Sci: Mater Electron (2008) 19:S371–S374
DOI 10.1007/s10854-008-9593-5

Investigation of defects in Cu(In,Ga)(S,Se)$_2$ films using the photocurrent decay technique

A. Saad · A. Odrinski · M. Tivanov · N. Drozdov · A. Fedotov · V. Gremenok · A. Mazanik · A. Patryn · V. Zalesski · E. Zaretskaya

Received: 27 September 2007 / Accepted: 18 January 2008 / Published online: 16 February 2008

Abstract In the present work we demonstrate the possibility of using the photoinduced current transient spectroscopy (PICTS) method to study the defects in Cu(In,Ga)(S,Se)$_2$ films which can be used as an absorber layer in solar cells (SCs). The conducted experiments enable one to determine the parameters (activation energies and effective capture cross-sections) of the defects revealed in the films under study.

A. Saad
Applied Science Department, Al-Balqa Applied University, Salt, Jordan

A. Odrinski
Institute of Technical Acoustics, National Academy of Sciences of Belarus, Lyudnikova av. 13, 210717 Vitebsk, Belarus
e-mail: odra@mail333.com

M. Tivanov · N. Drozdov · A. Fedotov · A. Mazanik (✉)
Belarusian State University, Nezavisimosti av. 4, 220050 Minsk, Belarus
e-mail: amazanik1@rambler.ru

M. Tivanov
e-mail: michael_bsu@yahoo.de

V. Gremenok · E. Zaretskaya
Joint Institute of Solid State and Semiconductor Physics, National Academy of Sciences of Belarus, P. Brovka str. 19, 220072 Minsk, Belarus
e-mail: ezaret@ifttp.bas-net

A. Patryn
Koszalin University of Technology, Sniadeckich str. 2, 75-453 Koszalin, Poland

V. Zalesski
Institute of Electronics, National Academy of Sciences of Belarus, Logoiski trakt str. 22, 220090 Minsk, Belarus

1 Introduction

The pentenary semiconductor Cu(In,Ga)(S,Se)$_2$ (CIGSS) is an excellent absorber material for heterojunction solar cells and modules on their basis [1, 2]. The band gap energies of CIGSS materials varying from 1.0 to 2.4 eV may be perfectly adjusted to the solar spectrum. Furthermore, the composition variations in depth of the absorber layer provide a means for band gap engineering and hence for improved device performance.

The creation of high-efficiency solar cells is impeded by the absence of information concerning the electrically active defects contained in the material and their influence on the device performance.

At present the photo-induced current transient spectroscopy (PICTS) method that is based on analysis of the temperature dependences of a transient photoresponse signal is effectively used to study deep level defects in highly resistive semiconductors [3, 4]. However, this method is practically unused for studies of the properties of CIGSS solid solutions forming absorber layers for high-efficiency and low-cost thin film solar cells. Though it is evident that a study into the influence of manufacturing technology on SCs efficiency necessitates knowledge of generation, capture and recombination mechanisms for the nonequilibrium charge carriers.

The main goal of this work is to apply the PICTS method for a study of deep level defects in the CIGSS solid solution films.

2 Experimental

Single-phase p-type CIGSS solid solution films have been prepared in two stages: (i) sequential deposition of Cu–In–Ga

precursors, and (ii) reactive annealing of these structures in S/Se-containing atmosphere under N_2 flow. The metallic precursors with a total thickness of about 1.0 μm were deposited onto the Corning glass 7059 substrate by ion-beam plasma evaporation in vacuum (6×10^{-4} Pa) at the substrate temperature $T_s = 100$ °C. The precursors reacted with elemental Se/S vapor under N_2 flow in a horizontal tube reactor at atmospheric pressure. At the first stage, the samples were heated for 10 min to the reaction temperature $T_1 = 250$ °C, and the initial reaction period was maintained at 20 min. Then the temperature was increased to $T_2 = 400$–540 °C at 9 °C min^{-1} and thereafter maintained invariable for 20 min. The samples were distinguished by S/(S + Se) ratio, varying from 0.44 to 0.88. An area of the samples was about 10×10 mm^2 and their thickness was approximately 2 μm.

The crystal structure of the samples was studied by the X-ray diffraction (XRD) method using a Siemens D-5000 diffractometer (Cu K_α $\lambda = 1.5418$ Å radiation, Ni filter) operated at 30 kV voltage and 20 mA current. The bulk composition of the films was investigated by wavelength dispersive X-ray (WDX) analysis using the CAMECA SX-100 apparatus.

For PICTS measurements the ohmic contacts were deposited on the film surface with the use of a silver paste. The distance between two coplanar contacts was 5 mm. The quality of these contacts was monitored regarding linearity of the current–voltage characteristics. Both the method and technique used in PICTS measurements were described in detail in [5]. The measurements were performed over the temperature range from 77 to 330 K with a temperature step 1 K and the sample heating rate of 2 K/min. The sample heating was realized using an automatically controllable current source and a resistance-type heater having a good thermal contact with the massive metallic plate where the sample was placed. The accumulation, averaging and file recording procedures for the photocurrent relaxation kinetics (usually about 50 times for each temperature point) were carried out during heating of the initially cooled sample. Each relaxation curve contained 2,000 points sampled in every fixed-time interval of 30–50 μs. Photoexcitation of the samples studied was done using monochromatic light corresponding to their maximal photosensitivity.

Analysis of the experimental data was performed according to the conventional DLTS procedure. For each temperature point a set of $P_j(T)$ spectra was calculated by the following equation:

$$P_j(T) = \int_0^\infty i(t,T) F_j(t)\,\mathrm{d}t \tag{1}$$

where $j = 1...8$—spectrum number, $i(t, T)$—signal of photocurrent relaxation recorded at temperature T, normalized to the steady-state photocurrent value and averaged over 50 realizations, $F_j(t)$—weight function defined as

$$F_j(T) = \begin{cases} 0, \ldots \text{when} \ldots t < \Delta t + \tau_j \\ +1, \ldots \text{when} \ldots \Delta t + \tau_j < t < \Delta t + 2\tau_j \\ -1, \ldots \text{when} \ldots \Delta t + 2\tau_j < t < \Delta t + 3\tau_j \\ 0, \ldots \text{when} \ldots t > \Delta t + 3\tau_j \end{cases}$$

where τ_j is the characteristic parameter for jth spectrum, Δt—temporary delay.

It is supposed that in the temperature range, where thermoemission from the nonequilibrium filled traps gives a significant contribution to the photocurrent relaxation, the temperature dependence of the function $i(t, T)$ may be expressed as

$$i(t,T) = f(t) + A\exp(-t/\tau_x(T))/\tau_x(T)$$

Here $f(t)$—temperature independent function describing relaxation of the nonequilibrium charge carriers, and the second-term corresponds to thermoemission from the nonequilibrium filled traps. The main contribution into the temperature dependence of thermoemission is given by the characteristic relaxation time of the nonequilibrium filled traps $\tau_x(T)$, and A is a constant. Parameter τ_x is inversely proportional the thermoemission rate as follows:

$$1/\tau_x = e^{\mathrm{th}} = \sigma v_{\mathrm{th}}\, N_c/g\exp(-E_t/kT),$$

where σ—apparent capture cross-section; $v_{\mathrm{th}} = (3kT/m_e^*)^{1/2}$—thermal velocity of charge carriers, m_e^*—effective mass of charge carriers, E_t—thermoactivation energy of traps, k—Boltzmann constant; $g = ½$—degeneration factor of a trapping level; $N_c = (2\pi m_e^* kT/h^2)^{3/2}$—effective density of the electronic states in the corresponding (valence or conductivity) band (h—Plank's constant). As a result, we obtain:

$$e^{\mathrm{th}}(T) = \sigma T^2 B\exp[-E_t/kT], \tag{2}$$

where B is a constant for the material studied. Taking into account expressions (1)–(3), one can show that relation

$$e_j^{\mathrm{th}} = \frac{1}{\tau_x} = \frac{1}{\tau_j}\ln\left[1 + \frac{2\tau_j}{\tau_j + \Delta t}\right] \tag{3}$$

is correct at maximum of $P_j(T)$ function.

The given characteristic relaxation times were ranging from 0.2 to 20 ms.

3 Results and discussion

As seen from the conducted experiments, there are two main maxima in the observed PICTS-spectra (Fig. 1). The first one (labeled as N1) is observed over the temperature

range 260–300 K, whereas the second one (labeled as N2)—for temperatures ranging 160–220 K.

The presence of these two maxima in the spectra is in a good agreement with the results obtained by the admittance-spectroscopy and DLTS methods in the solar cells with CIGSS absorber layers similar in compositions [6–11]. Therefore, the observed PICTS spectra confirm the presence of two deep traps for the charge carriers in the material under study.

By construction of a set of PICTS spectra $P_j(T)$, differing in the parameter τ_j, one can extract from maxima of the spectra a set of values for $(e^{th},T)_j$. Plotting the curves for $\ln[e^{th}/T^2]$ versus $1{,}000/T$ (Arrhenius scale), we can determine the thermoactivation energy E_t and effective capture cross-section σ of the charge carriers (See, Fig. 2).

The results for the N1-labeled traps are given in Fig. 2. It is seen that the curves are characterized by deviation from linearity suggesting the presence of several mechanisms of the photocurrent decay with different temperature dependences of the characteristic relaxation times.

The model used for interpretation of the results takes into account only the time dependence of the excess charge carrier concentration under periodical light excitation disregarding the diffusive carrier transport.

As our measurements of photovoltage have shown, the depletion region near the surface is characteristic for the studied p-type CIGSS films. This leads to accumulation of minority carriers (electrons) under photoexcitation, whereas the photogenerated holes remain within the bulk. According to [12], the mobilities of electrons and holes in CIGSS films differ by about an order of magnitude. After the illumination is switched off, diffusion of the electrons accumulated near the surface plays a significant part. The space separation of the photogenerated nonequilibrium charge carriers and their subsequent diffusion can lead to a distorted shape of the photocurrent relaxation curve. Inasmuch as the influence of diffusion is most significant for the initial part of the relaxation curve, a low-temperature part of Arrhenius plot up to the above mentioned nonlinearity deviation point was used for estimation of the defect parameters below.

The calculated values of the film parameters are listed in Table 1, where T—temperature range associated with registration of thermoemission from the traps, E_t—thermoactivation energy of the registered traps, and σ—effective capture cross-section of the respective charge carrier. To calculate the effective capture cross-section, we have used the effective hole mass 0.79 m_e and the effective electron mass 0.09 m_e, taken from the earlier work [12], where m_e—free electron mass.

As is seen from Table 1, the activation energies calculated from the approximation of linear parts of experimental data in the Arrhenius scale give the E_t values of about 350 meV for N1 traps and of about 120 meV for N2 traps. According to [13], N1 traps can be ascribed to the antisite defects (In_{Cu}) forming donor levels. According to [14, 15], N2 traps correspond to the vacancies in copper sublattice (V_{Cu}) which form acceptor levels. This is also confirmed by the elemental composition studies for the investigated films. As was shown, all the investigated films were copper-depleted and indium-enriched (see, Table 1). At the same time, the metal/chalcogenide ratio for all these films was nearly stoichiometric.

An analysis of Table 1 shows that the selenium ↔ sulfur substitution in CIGSS thin films has no evident influence both on the ensemble of defects dominant in the material and E_t and σ parameters for these defects.

A small values of the effective capture cross-sections σ indicate that nonequilibrium filling of N2 traps must occur mainly by direct optical excitation with photon absorption.

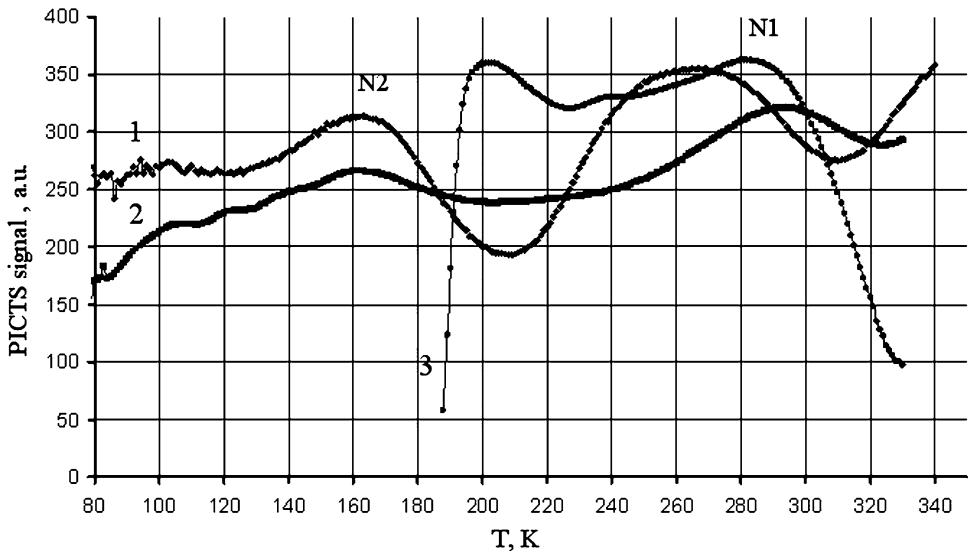

Fig. 1 The temperature dependence of PICTS signal: 1, $Cu_{0.73}In_{1.18}Ga_{0.09}S_{0.87}Se_{1.13}$; 2, $Cu_{0.82}In_{1.22}Ga_{0.04}S_{1.29}Se_{0.63}$; 3, $Cu_{0.81}In_{1.21}Ga_{0.06}S_{1.68}Se_{0.24}$; N1, N2—number of defects

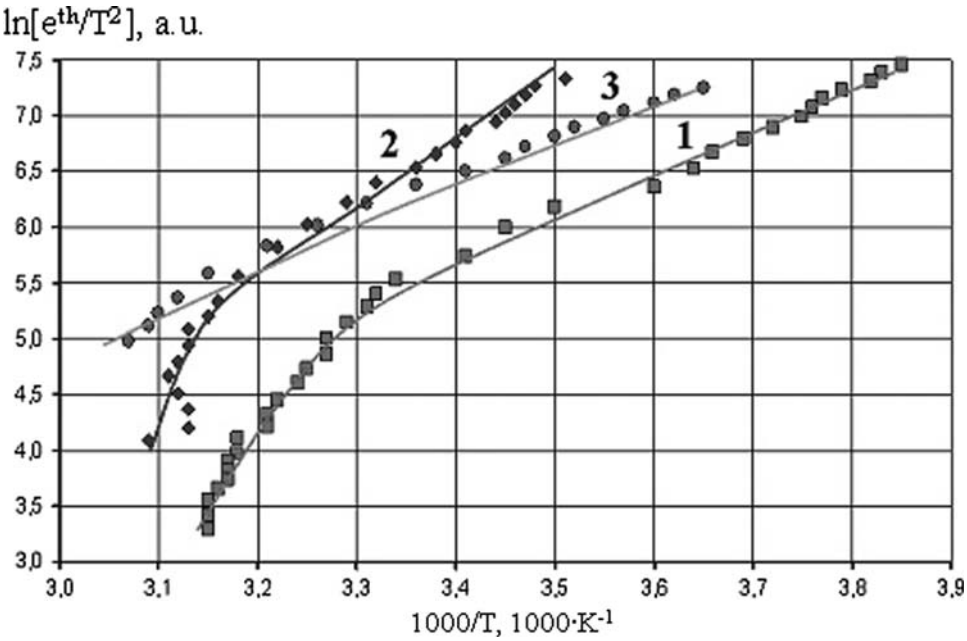

Fig. 2 The temperature dependence of the thermoemission rate e^{th}: 1, $Cu_{0.73}In_{1.18}Ga_{0.09}S_{0.87}Se_{1.13}$; 2, $Cu_{0.82}In_{1.22}Ga_{0.04}S_{1.29}Se_{0.63}$; 3, $Cu_{0.81}In_{1.21}Ga_{0.06}S_{1.68}Se_{0.24}$

Table 1 Thermoactivation energies E_t and effective capture cross-sections σ for N1 and N2 traps in the material studied

No.	Samples	N1 attributed to the antisite defects (In_{Cu})			N2 attributed to the copper vacancies (V_{Cu})		
	Molar fraction	T (K)	E_t (eV)	σ (cm^2)	T (K)	E_t (eV)	σ (cm^2)
1	$Cu_{0.73}In_{1.18}Ga_{0.09}S_{0.87}Se_{1.13}$	255–317	0.35	5×10^{-19}	151–227	0.12	1×10^{-20}
2	$Cu_{0.82}In_{1.22}Ga_{0.04}S_{1.29}Se_{0.63}$	285–320	0.42	7.7×10^{-18}	158–219	0.15	8×10^{-20}
3	$Cu_{0.81}In_{1.21}Ga_{0.06}S_{1.68}Se_{0.24}$	274–327	0.35	5×10^{-19}	176–214	0.12	4×10^{-21}

4 Conclusion

The proposed PICTS method makes it possible to study the carrier traps in CIGSS absorber films before the formation of a potential barrier. This study of the p-CIGSS thin films has revealed two types of defects which may be classed as antisite defects In_{Cu} and copper vacancies V_{Cu}.

The selenium ↔ sulfur substitution in CIGSS thin films has no evident influence on the ensemble of the dominant defects.

Acknowledgement This work was supported by research program "Crystalline and Molecular Structures" of Republic of Belarus and by VISBY Program of the Swedish Institute.

References

1. U. Rau, H.-W. Schock, J. Appl. Phys. A **69**, 131 (1999)
2. K. Ramanathan, M.A. Contreras, C.L. Perkins et al., Prog. Photovolt. Res. Appl. **11**, 225 (2003)
3. U. Rau, D. Braunger, R. Herbegholz, H.-W. Schock, J. Appl. Phys. **86**, 497 (1999)
4. L. Kronik, L. Burstein, M. Leibovitch, Y. Shapira, D. Gal, Appl. Phys. Lett. **67**, 1405 (1995)
5. I.A. Davydov, A.P. Odrinski, Electronics (in russian) **11**, 4 (1990)
6. T. Walter, R. Herberholtz, C. Muler, H.-W. Schock, J. Appl. Phys. **80**, 4411 (1996)
7. L.L. Kerr, S.S. Li, S.W. Johnston, T.J. Anderson, O.D. Crisalle, W.K. Kim, J. Abushama, R.N. Nou, Solid-State Electron. **48**, 1579 (2004)
8. M. Igalson, C. Platzer-Bjorkman, Sol. Energy Mater. Sol. Cells **84**, 93 (2004)
9. M. Turcu, I.M. Kötschau, U. Rau, J. Appl. Phys. A **73**, 769 (2001)
10. Z. Djebbour, A. Darga, A.M. Dubois, D. Mencaraglia, N. Naghavi, J.-F. Guillemoles, D. Lincot, Thin Solid Films **510–512**, 320 (2006)
11. M. Turcu, I.M. Kotschau, U. Rau, J. Appl. Phys. **91**, 1391 (2002)
12. S.M. Wasim, C. Rincon, G. Maryn, R. Marquez, J. Phys. Chem. Solids **64**, 1627 (2003)
13. P. Zabierowski, M. Edoff, Thin Solid Films **480–481**, 301 (2005)
14. J.J.M. Binsma, L.J. Giling, J. Bloem, J. Luminesc. **27**, 35 (1982)
15. H.Y. Ueng, H.L. Hwang, J. Phys. Chem. Solids **50**, 1297 (1989)